



# Migration Route Reconstruction of Different Cohorts of *Ommastrephes bartramii* in the North Pacific Based on Statolith Microchemistry

Peiwu Han<sup>1</sup>, Zhou Fang<sup>1,2,3,4,5\*</sup>, Nan Li<sup>1</sup> and Xinjun Chen<sup>1,2,3,4,5</sup>

<sup>1</sup> College of Marine Sciences, Shanghai Ocean University, Shanghai, China, <sup>2</sup> National Engineering Research Center for Oceanic Fisheries, Shanghai Ocean University, Shanghai, China, <sup>3</sup> Key Laboratory of Sustainable Exploitation of Oceanic Fisheries Resources, Ministry of Education, Shanghai Ocean University, Shanghai, China, <sup>4</sup> Key Laboratory of Oceanic Fisheries Exploration, Ministry of Agriculture and Rural Affairs, Shanghai, China, <sup>5</sup> Scientific Observing and Experimental Station of Oceanic Fishery Resources, Ministry of Agriculture and Rural Affairs, Shanghai, China

*Ommastrephes bartramii* is one of the important commercial fishery species in the North Pacific Ocean. It always migrates for a long distance in order to spawning and feeding. Understanding its migration route can be the basis for the sustainable development of the fisheries and scientific management of this species. Cephalopod statoliths contain a wealth of ecological information, which can provide useful information for studying spatio-temporal distribution. In this study, the statolith elements of winter-spring and autumn cohorts of *O. bartramii* in the North Pacific Ocean were measured by laser ablation inductively coupled plasma mass spectrometry (LA-ICP-MS). The differences in both composition and concentrations of elements between winter-spring and autumn cohorts were analyzed and the migration route were reconstructed. The analysis showed that the highest concentrations of elements in different cohorts was calcium (Ca). The concentrations of Ca, strontium (Sr), sodium (Na), iron (Fe), barium (Ba), and lithium (Li) showed significant differences between two cohorts ( $P < 0.01$ ). Mg, Ba, Sr, and Na were selected as the key elements in the two cohorts based on random forest method. Five clusters were obtained through chronological clustering, representing the five ontogenetic stages. Different cohorts selected different elements to fit the regression model with the corresponding water temperature. The high probability of occurrence in a particular area represented the possible optimal squid location based on a Bayesian model, and the potential migration routes of the different cohorts were reconstructed. This study shows that statoliths microchemistry can provide useful information for identifying the distribution and migration of oceanic squid.

**Keywords:** *Ommastrephes bartramii*, different cohorts, statolith, trace element, ontogenetic stage, migration route

## OPEN ACCESS

### Edited by:

Rui Rosa,  
University of Lisbon, Portugal

### Reviewed by:

Catalina Perales-Raya,  
Centro Oceanográfico de Canarias  
(IEO-CSIC), Spain  
Sílvia Lourenço,  
Instituto Politécnico de Leiria, Portugal

### \*Correspondence:

Zhou Fang  
zfang@shou.edu.cn

### Specialty section:

This article was submitted to  
Marine Biology,  
a section of the journal  
Frontiers in Marine Science

**Received:** 10 December 2021

**Accepted:** 09 February 2022

**Published:** 21 March 2022

### Citation:

Han P, Fang Z, Li N and Chen X  
(2022) Migration Route  
Reconstruction of Different Cohorts  
of *Ommastrephes bartramii*  
in the North Pacific Based on Statolith  
Microchemistry.  
*Front. Mar. Sci.* 9:832639.  
doi: 10.3389/fmars.2022.832639

## INTRODUCTION

Cephalopods are important marine economic species and occupy an important position in fisheries resources (Arkhipkin, 2013; Arkhipkin et al., 2021; Lishchenko et al., 2021). As both prey and active predator, cephalopods play an irreplaceable role within marine ecosystems (Santos et al., 2001; Lischka et al., 2020). Some of them have unusual life history characteristics: short life cycle, complex population structure, and long-distance migration (Jones et al., 2019). Understanding

migration route, connectivity and structure of a population is of great help to the protection and management of resources (Gillanders, 2005). Traditional techniques such as tagging are the most common methods used to study the migration of cephalopods (Wearmouth et al., 2013; Mereu et al., 2015). However, these techniques are difficult to implement on small species, because they are too fragile to be externally tagged. And cannibalism in squid and presence of predators, often resulting in loss of tags (Arkhipkin, 2005; Semmens et al., 2007; Jones et al., 2019). In recent years, geochemical analysis of hard tissue has been widely used in the study of cephalopod migration with the development of device and technology (Liu et al., 2016; Fang et al., 2019).

The statoliths of cephalopods are a pair of hard tissues within statocysts that grow continually throughout whole life (Radtke, 1983). Analogous to fish otoliths, cephalopod statoliths are mainly composed of inorganic substances (aragonite formed by calcium carbonate salt crystals) and organic substances (proteins) (Dilly, 1977). When cephalopods exchange substances with the external environment, the chemical elements in the environment enter the cephalopods body through respiration and ingestion, and then enter the endolymph through cell, finally deposit in the statoliths (Liu et al., 2011b). Each element concentration in the statoliths is related to the element affinity and chemical reactions during the deposition process (Xiong et al., 2015; Li et al., 2021). Once deposited, the components in the statoliths will not be changed (Campana and Neilson, 1985). Therefore, the elements absorbed into the statoliths can be permanently preserved (Liu et al., 2016; Li et al., 2021). Through the analysis of these elements, the environmental information in the life history of cephalopods can be effectively revealed (Liu et al., 2011a; Sun et al., 2015; Li et al., 2021). Yamaguchi et al. (2018) used the ratio of Sr/Ca in statolith to estimate the living water temperature of *Uroteuthis edulis*, and then combined with the inhabiting water layer, speculated that the spawning grounds of *U. edulis* caught in the Sea of Japan were in the southern of the East China Sea and the feeding grounds were in the southern of the Sea of Japan. Zumholz et al. (2007) found that *Gonatus fabricii* lived in sea surface during juvenile period and migrated into deeper waters during progressive maturation based on the changes of Ba/Ca ratio. In this same study, according to the increased ratio of Sr/Ca and U/Ca from the nucleus to the edge of the statolith, *G. fabricii* was found to move to colder water as their growth (Zumholz et al., 2007). In addition, Liu et al. (2016) used the ratio of Sr/Ca and Ba/Ca of statoliths and combined with sea surface temperature (SST) to successfully establish the migration route of *Dosidicus gigas* from juvenile to adult stage. Therefore, the ratios of trace elements in statoliths to Ca can be used as an important indicator for studying population migration and habitat.

Neon flying squid, *Ommastrephes bartramii*, is an oceanic cephalopod, which is widely distributed in temperate and subtropical waters (Murata, 1990; Yu et al., 2015; Fang et al., 2021). Its commercial exploitability and utilization are mainly concentrated in the North Pacific Ocean (Yu et al., 2016). China mainland started commercial fishing in 1994 and is currently one of the main countries for catching this species, with an annual yield of 60,000–100,000 tons in recent two decades (Chen et al.,

2008). As a key fisheries species, *O. bartramii* is involved in the transfer of inorganic and organic substance across various parts of the ecosystem and plays an important role in the food web (Watanabe et al., 2004). It is an important food source for large predators, and it also preys on crustaceans, small pelagic fish, and other cephalopods (Bower and Ichii, 2005; Alabia et al., 2020). Thus, understanding the life history process of *O. bartramii* is also a prerequisite to ensure the health of ecosystem.

The population structure of *O. bartramii* has been discussed in some studies (Murata, 1990; Bower and Margolis, 1991; Chen and Chiu, 2003). At present, there are evidences that we could accept that exists two segregated cohorts; the winter-spring cohort that is mainly distributed west of 170°E (Western stock) with peak hatching periods from January to April and the autumn cohort located east of 170°E (Eastern stock) with peak hatching periods from September to November, both of which have an annual lifespan (Yatsu et al., 1997; Bower and Ichii, 2005; Fang et al., 2016a,b). *O. bartramii* migrates for a long distance from south to northern waters to feed and spawn (Fang et al., 2019). However, the two cohorts have different migration routes, which cause them to experience different ocean conditions, then resulting in asynchronous growth patterns and varied abundances (Chen and Chiu, 2003; Chen, 2010; Fang et al., 2016a). Therefore, in order to understand the life history and biological characteristics of different cohorts of *O. bartramii*, it is necessary to study their migration routes.

In this study, we determined the main trace elements in the statoliths of different cohorts of *O. bartramii* based on laser ablation inductively coupled plasma mass spectrometry (LA-ICP-MS). Then we analyzed the differences in the composition and concentration of trace elements in statoliths, and explored the changes and differences of the ratios of key trace elements to Ca in the time series. Finally, according to the relationship between water temperature and trace elements in statoliths, the migration routes of different cohorts of *O. bartramii* were reconstructed. This study can provide scientific reference for revealing the life history of different cohorts of *O. bartramii* in the North Pacific Ocean.

## MATERIALS AND METHODS

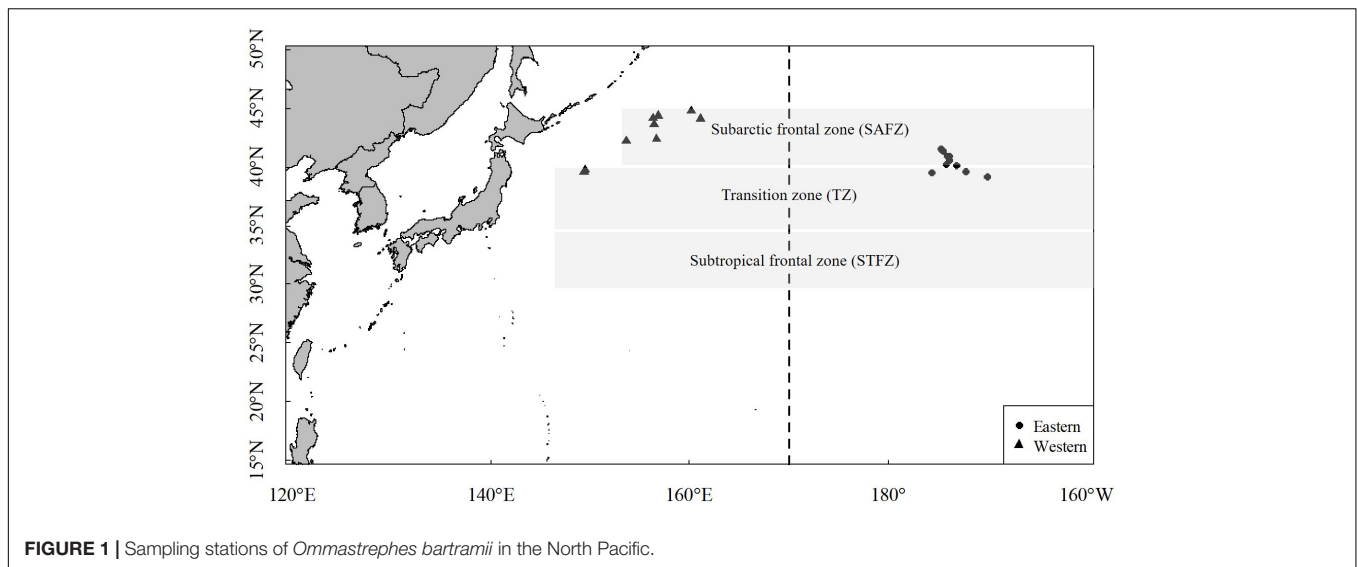
### Sampling and Measurement

A total of 80 squid samples were randomly collected from the Chinese commercial jigging vessel on two main fishing grounds (149°E–168°W, 39–45°N) in the North Pacific Ocean from May to November in 2020 (Figure 1). Samples were immediately frozen at  $-20^{\circ}\text{C}$  on the vessel and transported to laboratory for subsequent biological analysis.

Samples were measured after thawing in the laboratory, including dorsal mantle length (ML,  $\pm 1$  mm) and body weight (BW,  $\pm 1$  g), and visually assessed for sex and maturity stage according to Lipinski and Underhill (1995).

### Age Estimation and Back-Calculation

The statoliths were extracted from statocysts of all *O. bartramii*, then numbered and put into 1.5-mL centrifuge tube filled with



75% ethanol to clean (Liu et al., 2011a,b). Embedding, grinding, polishing and photographing of statoliths were carried out according to Liu et al. (2011a,b). Daily increments were based on the validated age of ommastrephid squids (Hu et al., 2015; Wang et al., 2021). The age was estimated by counting daily growth increments along the sagittal section from the first increment outside the core to the last increment near the margin of the statolith along the same axis (**Figure 2**) (Wang et al., 2021). Increments of each statolith were counted twice by different readers and counts were not accepted until the difference between the counts of two readers was less than 5% (Liu et al., 2011a,b).

The hatching date of *O. bartramii* was back-calculated by estimated age and the date of capture. Based on hatching date, samples from different areas were assigned to their spawning cohort. The eastern stock and western stock belong to autumn cohort and winter-spring cohort, respectively (**Table 1**).

### Trace Element Analysis in Statoliths

All statoliths were analyzed using LA-ICP-MS in Key Laboratory of Sustainable Development of Fishery Resources of the Ministry of Education, Shanghai Ocean University. The laser ablation system is UP-213, and the ICP-MS is Agilent 7700x. In the laser ablation process, Helium is used as the carrier gas, and Argon is used as the compensation gas to adjust the sensitivity (Hu et al., 2008). In order to reduce the interference caused by contaminants to the element test, the polished statolith slices were washed in deionized water (resistivity > 18 MΩ) for 5 min and dried in a Class-100 laminar flow column. Four glass standard materials BHVO-2G, BCR-2G, BIR-1G, and SRM610 were used for standard calibration. The time period of each data analysis included approximately 20 s blank signal and 50 s sample signal (Fang et al., 2019, **Table 2**).

The method of equidistant ablations was adopted. From the core to the edge of statolith, ablation spots of 30 μm diameter were located at 50 μm intervals (**Figure 2**). The number of ablation spots ranged from 12 to 17 per statolith. Eight elements

(<sup>7</sup>Li, <sup>23</sup>Na, <sup>43</sup>Ca, <sup>55</sup>Mn, <sup>57</sup>Fe, <sup>63</sup>Mg, <sup>88</sup>Sr, and <sup>137</sup>Ba) were quantified at each ablation spot. The processing of the elements was carried out using ICPMSDataCal software (Liu et al., 2008).

### Environmental Data

This study selected SST and Temp\_100 water temperature to analyze the migration of two cohorts. Many studies had shown that the ratio of elements to Ca in statolith has a certain relationship with temperature (Zumholz et al., 2007; Liu et al., 2016; Yamaguchi et al., 2018). In addition, the vertical distribution of water temperature also affects the water layer where squid inhabit and migration of individual, thus influences the deposition of statolith elements (Liu et al., 2015; Li et al., 2021). Previous studies have shown that *O. bartramii* inhabited the sea surface in the early life history, and the SST determined the most suitable spawning ground (Yu et al., 2013; Fang et al., 2019). After maturing, the growth of *O. bartramii* has a good correlation with the water temperature of 100 m (Temp\_100) (Han et al., 2022; Wang et al., 2022).

The weekly SST and Temp\_100 data were obtained from NOAA High-resolution Blended Analysis<sup>1</sup> with spatial resolution of 0.5° × 0.5°. The time range of all download environmental data was April 2019–December 2020, and the space range was 20–50°N and 120°E–140°W. The water temperature that were closest to the ontogeny stage within a week were considered as the water temperature of the life history stage.

### Statistical Analysis

One-way analysis of variance (ANOVA, significant level α = 0.05) was used to test the differences in the concentrations of eight trace elements in the winter-spring and autumn cohorts (Li et al., 2021). The random forest method was used to select the key elements of the winter-spring and autumn cohorts for the ratio of Ca (Pan et al., 2020). Two-way analysis of variance was used to

<sup>1</sup><http://apdrc.soest.hawaii.edu/las/v6>

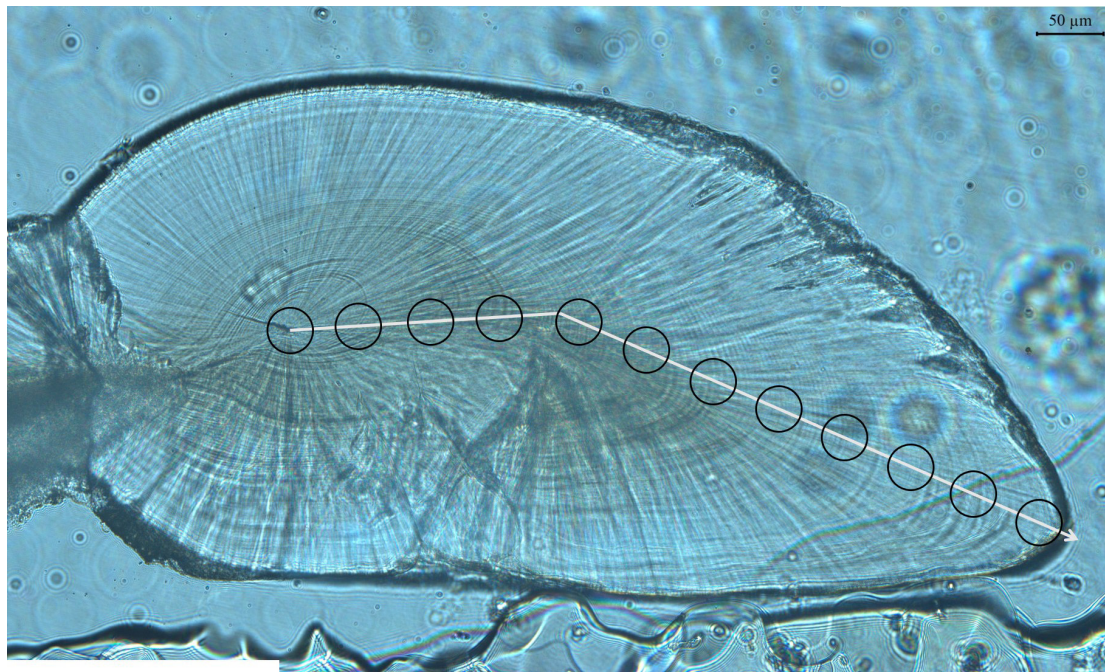


**FIGURE 2** | Image of statolith. Line indicates the direction of age estimation and ablation (from the central nucleus to the rostrum edge). Circles indicate regions where material has been ablated.

**TABLE 1** | Data of statolith samples tested by the microchemical analysis of *Ommastrephes bartramii*.

Area	Month	Locations	N	Mantle length/mm	Age range (days)	Sex ratios (Male : Female)	Hatching month
Eastern	May 2020	169°59'W–175°36'W; 39°09'N–40°09'N	10	300–407	201–294	0:1	August–October
	June 2020	173°52'W–175°25'W; 40°25'N–40°55'N	15	345–463	241–308		August–September
	July 2020	174°14'W–174°29'W; 40°16'N–41°23'N	5	367–501	255–346		August–October
Western	August 2020	156°40'E; 42°25'N	8	257–347	157–248	1:2	January–February
	September 2020	161°04'E–160°11'E; 44°06'N–44°47'N	14	276–322	189–226		February–March
	October 2020	156°20'E–156°50'E; 44°10'N–44°23'N	14	270–394	191–281		January–March
	November 2020	149°22'E–149°30'E; 39°34'N–39°44'N	14	342–397	237–297		February–March

N, number of samples collected.

test the differences in the ratio of key elements to Ca in different cohorts and different distances from core of statolith. Based on the ratio of key elements to Ca, the multivariate regression tree (MRT) model was established (Pan et al., 2020). According to the results of MRT, the different cohorts of *O. bartramii* were divided into five ontogenetic stages, which are embryonic stage, paralarval stage, juvenile stage, sub-adult stage, and adult stage.

By merging the ablation spots of ontogenetic stages, the age of each ontogenetic stage could be obtained. The timing of each ontogenetic stage can be estimated by adding the date of hatching and the corresponding age.

All statistical analyses were performed with R 3.3 (R Development Core Team, 2019).

## Hypothesis and Assumptions

The stepwise multiple linear regression method was used to analyze and establish the relationship between key trace elements and Temp<sub>100</sub> in different cohorts. And the optimal model

was selected according to the Akaike information criterion (AIC) (Akaike, 1974, **Supplementary Table 1**). Based on the hypothetical relationship between Temp<sub>100</sub> and related elements, we were able to find the optimal Temp<sub>100</sub> for the later ontogenetic stage (sub-adult stage and adult stage) according to the elements concentration of squid statolith in

**TABLE 2** | Analytical parameters of laser ablation inductively coupled plasma mass spectrometry (LA-ICP-MS).

Parameters of laser UP-213		Parameters of Agilent 7700x ICP-MS	
Wave length	193 nm	Frequency of RF	1,350 W
Energy density	8.0 J/cm <sup>-2</sup>	Speed of plasma	Ar (15 L/min <sup>-1</sup> )
Sample gas	He(0.65 L/min <sup>-1</sup> )	Speed of added gas	Ar (1.0 L/min <sup>-1</sup> )
Spot diameter	30 µm	Complement gas	Ar (0.7 L/min <sup>-1</sup> )
Frequency	5 Hz	Depth of spot	5 mm
Spot method	Spot	Mode of detector	Dual

**TABLE 3** | Element concentration in statolith of winter-spring and summer cohorts of *Ommastrephes bartramii*.

Cohort	Element	Concentration (ppm)			Cohort	Element	Concentration (ppm)			Significance
		Min	Max	Mean ± SD			Min	Max	Mean ± SD	
Autumn cohort	Ca	407198.36	409385.05	408295.27 ± 402.33	Winter-spring cohort	Ca	402789.02	409209.83	408114.58 ± 476.70	$P < 0.00$
	Sr	5407.12	7733.18	6280.01 ± 446.12		Sr	5274.13	7891.49	6130.17 ± 463.16	$P < 0.00$
	Na	3717.46	5478.50	4744.89 ± 328.05		Na	3874.14	6309.13	4976.37 ± 351.22	$P < 0.00$
	Fe	45.94	503.65	105.00 ± 74.51		Fe	63.63	527.86	167.48 ± 87.72	$P < 0.00$
	Mg	19.65	287.66	58.52 ± 43.72		Mg	22.44	290.68	58.20 ± 44.44	$P > 0.05$
	Ba	1.31	12.25	5.66 ± 1.97		Ba	1.89	10.98	5.26 ± 1.63	$P < 0.00$
	Mn	0.05	70.49	4.28 ± 7.66		Mn	0.05	91.32	4.71 ± 9.60	$P > 0.05$
	Li	0.02	1.83	0.77 ± 0.39		Li	0.02	2.58	0.84 ± 0.42	$P < 0.00$

later life stage. The possible spatial locations corresponding to the optimal Temp\_100 can be determined according to the identified elemental concentration (Liu et al., 2016; Fang et al., 2019). Taking into account the squid swimming ability, the Bayesian model was used to find the possible location (longitude and latitude) of Temp\_100 from the Temp\_100 database mentioned previously.

According to the predicted location of the sub-adult stage (the highest probability of occurrence), combined with the corresponding date and elements concentration, the stepwise multiple linear regression method was used to analyze and establish the relationship between key trace elements and SST in different cohorts. And the optimal model was selected according to the AIC (Akaike, 1974, **Supplementary Table 2**). Based on the hypothetical relationship between SST and related elements, we were able to find the optimal SST for the earlier ontogenetic stage (embryonic stage, paralarval stage, and juvenile stage) according to the elements concentration of squid statolith in different life stage (Liu et al., 2016; Fang et al., 2019).

Squid in the same cohorts are likely to inhabit the same habitat and experience a similar environment during each ontogenetic stage, even though their hatching dates were different (Liu et al., 2016; Fang et al., 2019). Ultimately, the possible migration routes of different cohorts of *O. bartramii* were connected by combining the predicted optimal locations at all five ontogenetic stages. The squid were assumed to swim in a range of defined suitable SST values, and the maximum swimming speed of *O. bartramii*, 20 km per day (Tanaka, 2001), was used for calculating the possible migration range (Fang et al., 2019). The possibility of a squid occurrence area was also calculated following Liu et al. (2016).

## RESULTS

### Element Concentration and Screening of Key Elements of Different Cohorts in Statolith

Among the element concentrations of different cohorts in statolith, the highest concentration was calcium (Ca) which reached  $408114.58 \pm 476.70$  ppm in winter-spring cohort and  $408295.27 \pm 402.33$  ppm in autumn cohort

(**Table 3**). Strontium (Sr) had the second highest concentration with  $6130.17 \pm 463.16$  ppm in winter-spring cohort and  $6280.01 \pm 446.12$  ppm in autumn cohort. The order of the concentration of other elements of different cohorts was consistent from high to low, all are: sodium (Na) > iron (Fe) > magnesium (Mg) > barium (Ba) > manganese (Mn) > lithium (Li). ANOVA results showed that the concentrations of Ca, Sr, Na, Fe, Ba, and Li were significantly different between winter-spring and autumn cohorts ( $P < 0.01$ ), while there are no significant differences between the two cohorts of the concentrations of Mg and Mn ( $P > 0.05$ ).

According to the random forest results, four elements (Mg, Sr, Ba, and Na) were selected as the key elements affecting the trace element composition in statoliths of two cohorts (**Figure 3**), which were then used for subsequent analysis. In contrast, Mn, Fe, and Li were relatively unimportant (increase in MES less than 20%, **Figure 3**), which were not used for subsequent analysis.

### The Ratio of Key Elements to Calcium

The results showed that the ratio of Mg/Ca in the two groups showed a decreasing trend. From the core to 150  $\mu\text{m}$ , the ratio of Mg/Ca decreased sharply, and then decreased slowly. The Mg/Ca ratio of the autumn cohort was higher than that of the winter-spring cohort from the core to 450  $\mu\text{m}$ . After 450  $\mu\text{m}$ , the Mg/Ca ratio of the two cohorts was close (**Figure 4**). Accordingly with ANOVA results, the ratio of Mg/Ca had significant differences between winter-spring and autumn cohort ( $P < 0.05$ ), and also had significant differences in Mg/Ca at different stages ( $P < 0.01$ ).

The Ba/Ca ratio of the two cohorts firstly decreased slowly, then increased. Before 600  $\mu\text{m}$ , the Ba/Ca ratio of the two cohorts was similar. While between 650 and 750  $\mu\text{m}$ , the Ba/Ca ratio of the winter-spring cohort was slightly higher than the autumn cohort (**Figure 4**). Accordingly with ANOVA results, the ratio of Ba/Ca had no significant differences between winter-spring and autumn cohort ( $P > 0.05$ ), and had significant differences in Ba/Ca at different stages ( $P < 0.01$ ).

The Sr/Ca ratio of the two cohorts both showed a “U” trend. It showed a downward trend from the core to 400  $\mu\text{m}$ , and then gradually increased after 400  $\mu\text{m}$ . From the core to 100  $\mu\text{m}$ , the Sr/Ca ratio of the winter-spring cohort was similar to that of the autumn cohort. While after 200  $\mu\text{m}$ , the Sr/Ca ratio of the autumn cohort was greater than that of the winter-spring cohort

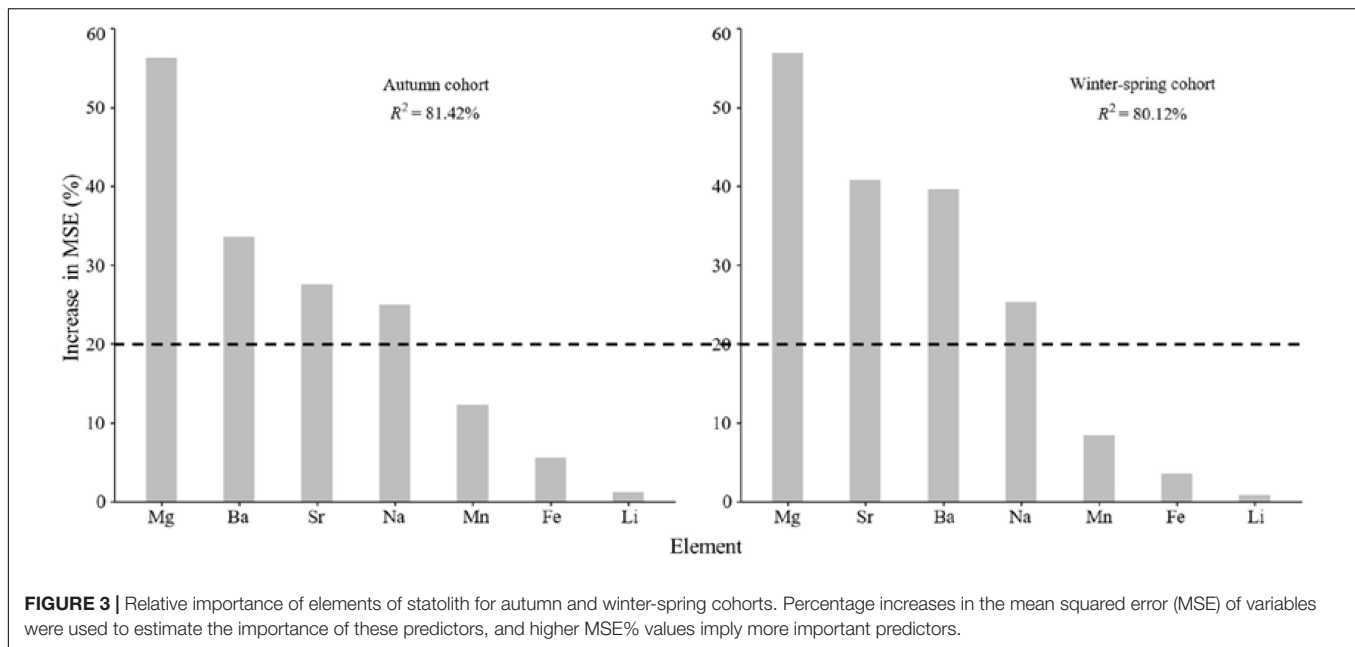


(Figure 4). Accordingly with ANOVA results, the ratio of Sr/Ca had significant differences between winter-spring and autumn cohort ( $P < 0.01$ ), and also had significant differences in Sr/Ca at different stages ( $P < 0.01$ ).

The curve of Na/Ca ratio of two cohorts was similar, showing a “M-shape.” At all stages, the Na/Ca ratio of the autumn cohort was lower than that of the winter-spring cohort (Figure 4). Accordingly with ANOVA results, the ratio of Sr/Ca had significant differences between winter-spring and autumn cohort ( $P < 0.01$ ), and also had significant differences in Sr/Ca at different stages ( $P < 0.01$ ).

### Multivariate Chronological Clustering

The results show that there were four critical points separated from the core to the edge of statolith which divided the whole life history into five clusters, and since the distance between each cluster is different, the number of ablation spots in each cluster was also different (Figures 5, 6).

In the Cluster 1, the two cohorts both contained one ablation spot, and the corresponding age was 0 day. In the Cluster 2, the two cohorts both contained three ablation spots, and the corresponding average ages were 30 days (autumn cohort) and 26 days (winter-spring cohort). In the Cluster 3, the autumn cohort contained four ablation spots and the winter-spring cohort contained three ablation spots, and the corresponding average ages were 74 and 60 days, respectively. In the Cluster 4, the two cohorts both contained four ablation spots, and the corresponding average ages were 134 days (autumn cohort) and 109 days (winter-spring cohort). In the Cluster 5, the autumn cohort contained 2~5 ablation spots and the winter-spring cohort contained 1~4 ablation spots, and the corresponding minimum ages were 181 and 145 days, respectively.

Based on the age, growth, and life history of *O. bartramii* (Chen and Chiu, 2003; Fang et al., 2019), the five cluster in

this study were defined as five ontogenetic stages. Cluster 1 represented embryonic stage, Cluster 2 represented paralarval stage, Cluster 3 represented juvenile stage, Cluster 4 represented sub-adult stage, and Cluster 5 represented adult stage (Table 4).

### Migration Route Reconstruction

According to the result of stepwise regression analysis, the optimal regression relations were expressed as follows:

$$\text{Temp}_{100\text{autumn cohort}} = 13.773 + 1.205 \times 10^{-2} \times \text{Mg}/\text{Ca} - 1.688 \times 10^{-4} \times \text{Sr}/\text{Ca} (R^2 = 0.78, P < 0.05)$$

$$\text{SST}_{\text{autumn cohort}} = 22.56 - 0.709 \times \text{Ba}/\text{Ca} + 2.940 \times 10^{-2} \times \text{Mg}/\text{Ca} (R^2 = 0.76, P < 0.01)$$

$$\text{Temp}_{100\text{winter-spring cohort}} = 108.671 - 6.827 \times 10^{-3} \times \text{Sr}/\text{Ca} + 0.167 \times \text{Ba}/\text{Ca} (R^2 = 0.84, P < 0.01)$$

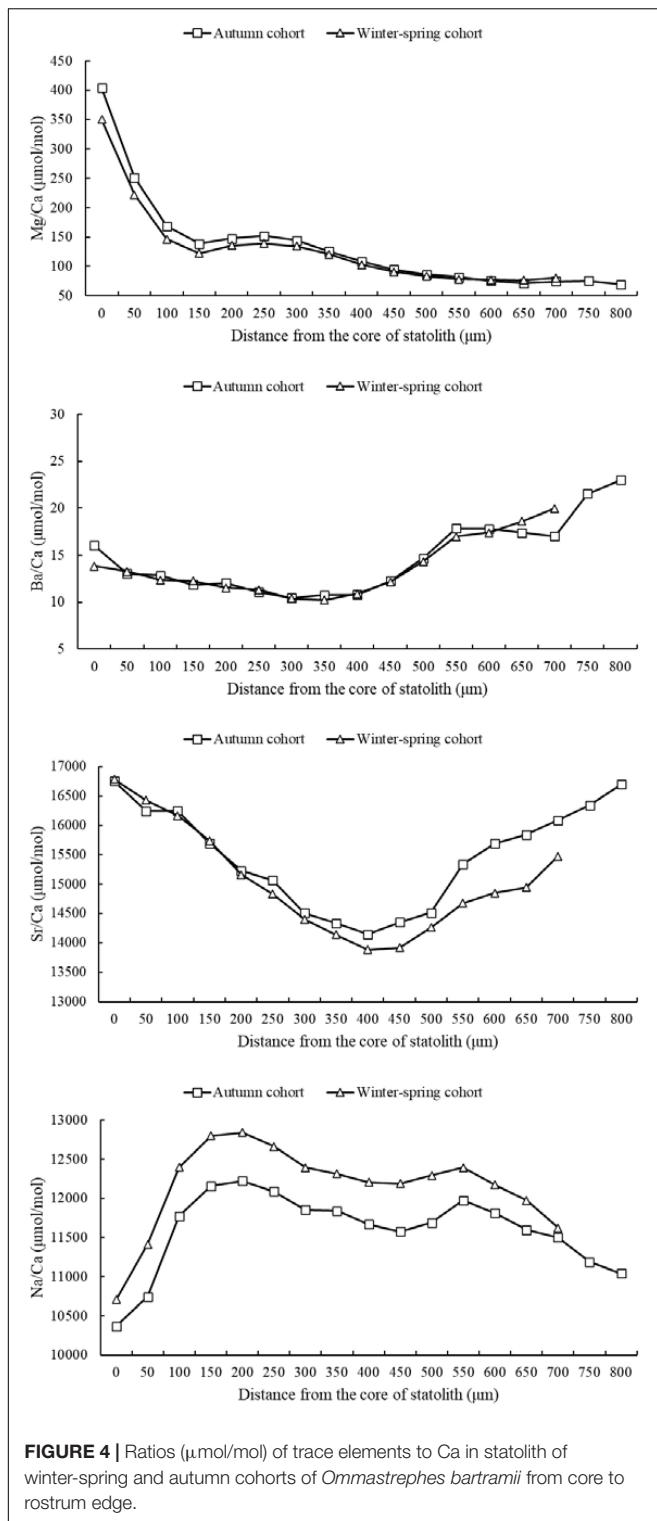
$$\text{SST}_{\text{winter-spring cohort}} = 15.845 - 1.292 \times 10^{-4} \times \text{Sr}/\text{Ca} - 0.133 \times \text{Ba}/\text{Ca} + 2.120 \times 10^{-2} \times \text{Mg}/\text{Ca} + 3.652 \times 10^{-4} \times \text{Na}/\text{Ca} (R^2 = 0.79, P < 0.01)$$

The occurrence probability of different cohorts of *O. bartramii* at different ontogenetic stages was calculated and the results are shown in Figures 7, 8.

## DISCUSSION

### Cohorts Variation of Elements

More than 50 elements have been detected in squid statoliths so far (Lu et al., 2013, 2014, 2015, 2019). In this study, eight main elements were studied and analyzed. Statoliths are



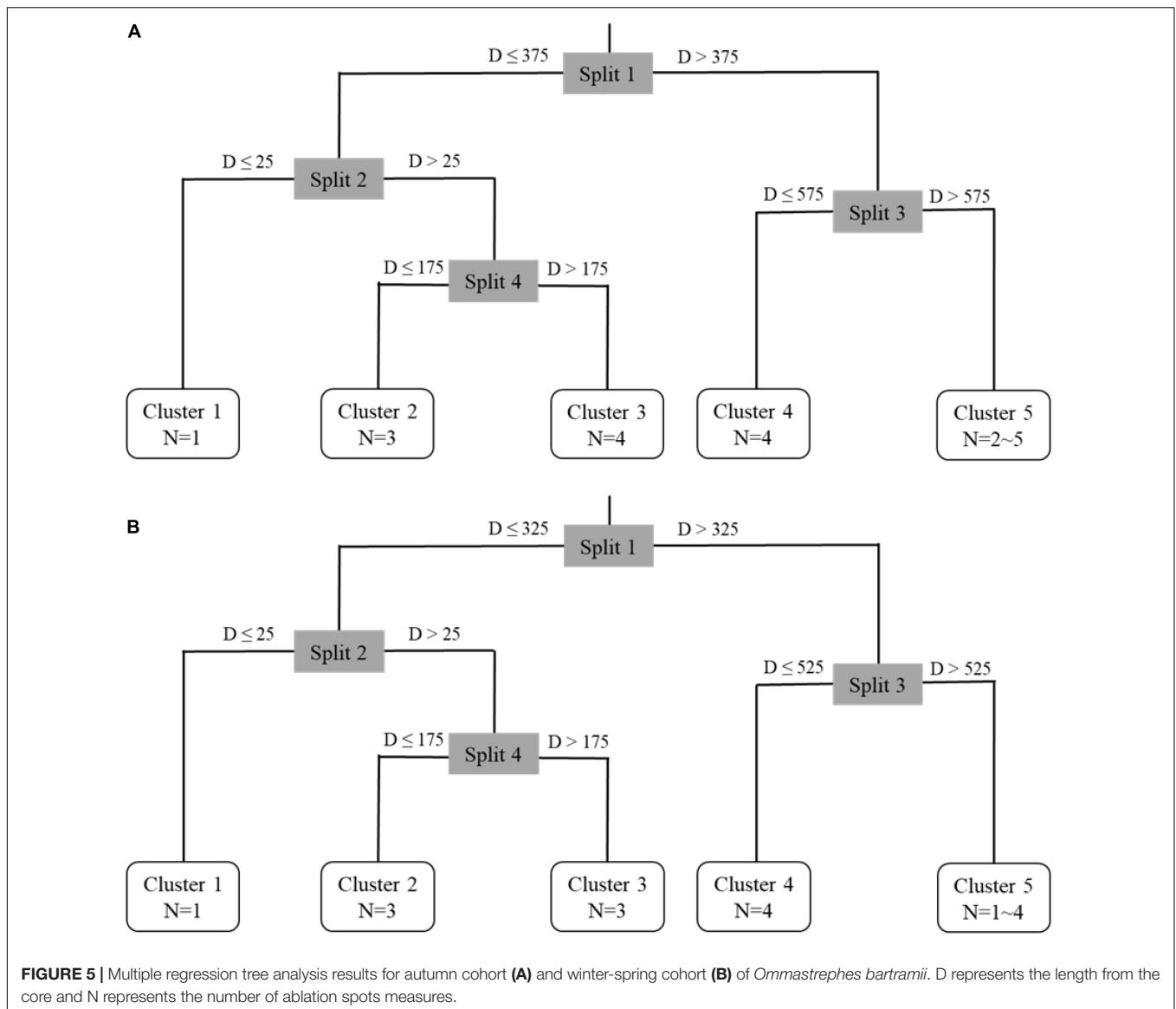
calcareous tissues, and the main component is calcium carbonate, which accounts for more than 95% of the entire statoliths (Liu et al., 2011b). Therefore, the concentration of Ca in spring-winter and autumn cohorts was the highest. In addition, the concentration of Sr was the second place in two cohorts, and this

phenomenon also occurs in some other ommastrephid squid, like *D. gigas* (Liu et al., 2011a; Lu et al., 2013), *Illex argentinus* (Lu et al., 2015), and *Stheno euthis oualaniensis* (Lu et al., 2019), which may be related to the element affinity in statoliths (Gillanders et al., 2013). During the formation of statoliths, hard acid ions are easy to enter the statoliths, especially for elements of the homologous element of Ca. The ionic radius of Sr is close to that of Ca. During the deposition of calcium carbonate, Sr ions replace Ca ions into the statoliths, therefore which leading to a higher concentration of Sr element in statoliths (Arkhipkin, 2005). Among these eight elements, except for Mg and Fe, other elements concentration had significant differences in the spring-winter and autumn cohorts. Studies have shown that differences in sea temperature, food sources, and salinity affect the deposition of trace elements in statoliths (Xiong et al., 2015; Li et al., 2021). The migration routes of the spring-winter and autumn cohorts are different, and the habitat environment at each ontogenetic stage is also different, which may cause the difference in element concentration (Fang et al., 2016a; Han et al., 2022).

Our results show that Mg, Ba, Sr, and Na are key elements to discriminate the statoliths microchemistry between the two cohorts. Mg element is a co-factor of adenosine triphosphate (ATP) and contributes to the phosphorylation of enzymes, and plays an important role in the biomineralization of statoliths (Hüssy et al., 2020). Ba element is one of the important “labels” indicating changes in the marine environment, which is usually regarded as an indicator element of upwelling and vertical movement of cephalopods (Zumholz et al., 2007). Sr element is an indispensable element in the deposition process of statoliths, which indicates the changes in salinity and temperature of the squid habitat, and also controls the swimming behavior of individual (Gillanders et al., 2013; Li et al., 2021). Na element indicates the physiological characteristics of the individual (Lu et al., 2014; Xiong et al., 2015). Therefore, the concentration of these elements can not only mirror the life course of the individual, but also reflect the changes in the habitat water environment.

## Key Elements to Calcium Ratios in Different Cohorts

The ratios of different elements to Ca in statoliths can objectively reflect the changes in the habitat environment during the growth of cephalopods, and these ratios are an effective tool for reversing their life history and reconstructing migration route (Liu et al., 2016; Li et al., 2021). This study found that the Mg/Ca ratio of the winter-spring and autumn cohorts both showed a downward trend throughout the whole life cycle. Mg element is believed to play an important role in the biomineralization of statoliths (Morris, 1991). Its concentration is related to the deposition of organic substance in statoliths (Bettencourt and Guerra, 2000). As the individual grows, the proportion of organic substance in statoliths decreases (Bettencourt and Guerra, 2000), and the concentration of Mg in statoliths also gradually decreases. Arkhipkin et al. (2004) found that the Mg/Ca ratio of statoliths of *Doryteuthis gahi* also had a similar trend, the statoliths of



immature individuals contained higher Mg/Ca ratio, while the statoliths of mature individuals contained lower Mg/Ca ratio. Zumholz et al. (2007) indicated the Mg/Ca ratio of *G. fabricii* gradually decreased from the core to the edge of statoliths, and believed that this result was related to the growth rate of the statoliths. Therefore, the distribution pattern of Mg/Ca ratio may reflect the growth process of the individual. Studies by Liu et al. (2011a) and Xu et al. (2020) had shown that Mg/Ca ratio could discriminate between different geographic populations of *D. gigas*. Similarly, in this study, it was found that there are differences in Mg/Ca ratio between winter-spring and autumn cohorts, especially in the core area (embryonic stage). Therefore, this difference can also provide a basis for the population division of *O. bartramii*. The Ba/Ca ratio increases with the increase of water depth, and is considered to be an important indicator of the vertical movement of squid (Chan et al., 1997; Liu et al., 2013). The Ba/Ca ratio of the two cohorts first

decreased slowly and then increased rapidly with the growth of the individual, which is consistent with the distribution of Ba/Ca ratio of *D. gigas* (Liu et al., 2011a). In nature, ommastrephids lay gelatinous egg mass (with thousands of eggs) which generally remain at certain depths according to their density (O'Dor and Balch, 1985; Ichii et al., 2009; Vijai et al., 2015). Hatched paralarvae from the floating egg mass gradually ascend to the surface waters, and individuals move to deeper waters layer during the progressive maturation (Liu et al., 2011a; Vijai et al., 2015). Therefore, the change of Ba/Ca ratio of *O. bartramii* and *D. gigas* may be caused by the change of habitat water layer at different stages.

The change of Sr/Ca ratio in the two cohorts showed a "U" trend, which was consistent with the results of previous studies (Yatsu et al., 1998). Many studies have shown that the Sr/Ca ratio has a negative correlation with water temperature (Zumholz et al., 2007; Liu et al., 2016; Yamaguchi et al., 2018).

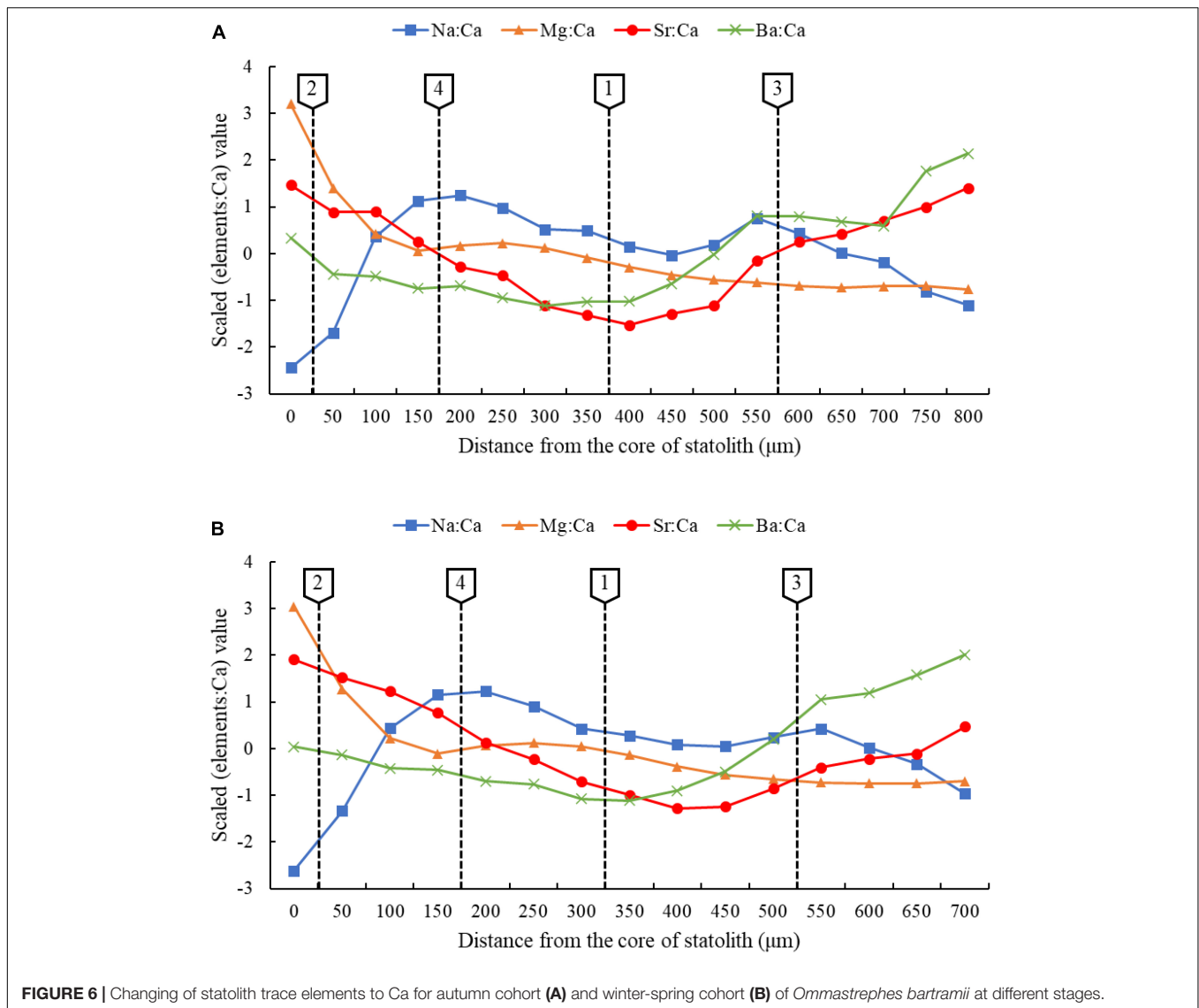


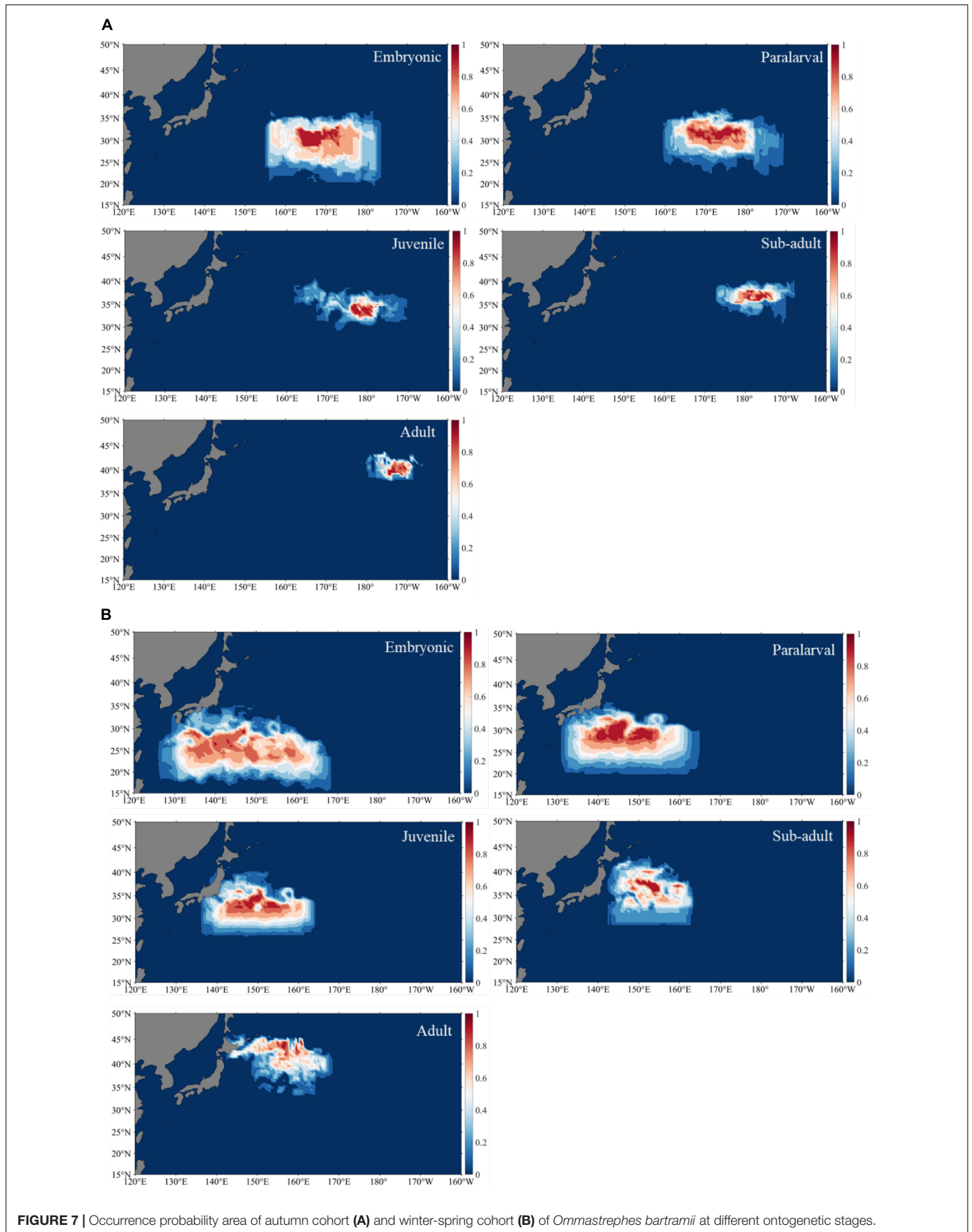
**FIGURE 6 |** Changing of statolith trace elements to Ca for autumn cohort (A) and winter-spring cohort (B) of *Ommastrephes bartramii* at different stages.

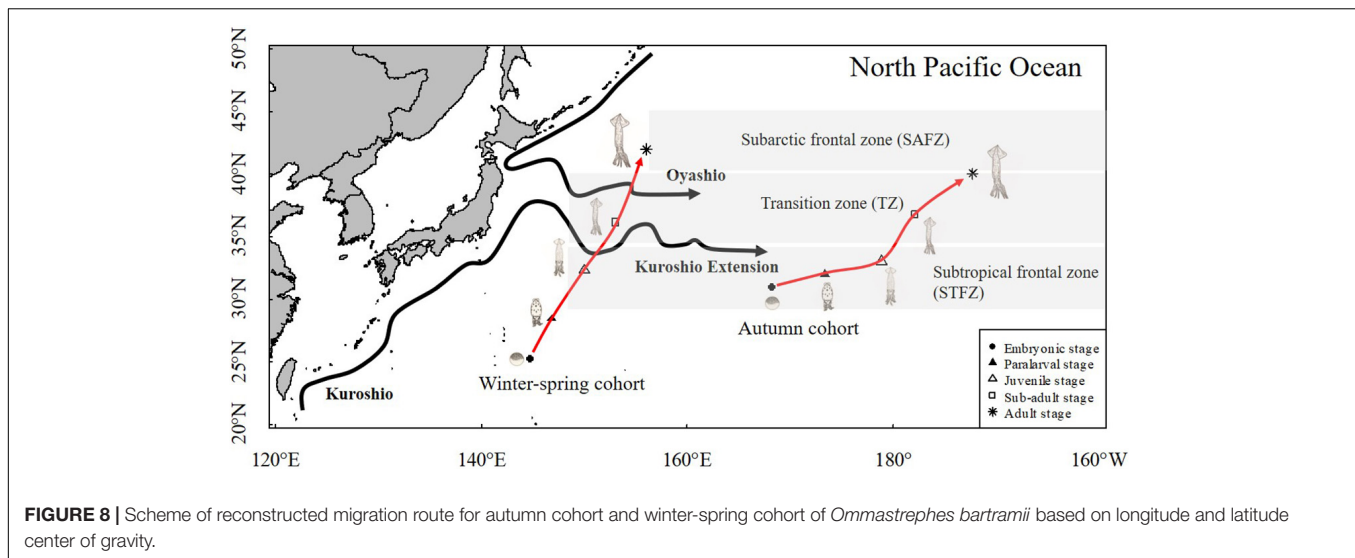
**TABLE 4 |** The summary of distance from the core, ontogenetic stage, and elemental ratios ( $\mu\text{mol/mol}$ ) for each cluster of different cohorts.

Cohort	Cluster number	Distance from the core ( $\mu\text{m}$ )	Ontogenetic stage	Na:Ca Mean $\pm$ SD	Mg:Ca Mean $\pm$ SD	Sr:Ca Mean $\pm$ SD	Ba:Ca Mean $\pm$ SD
Autumn cohort	1	D $\leq$ 25	Embryonic stage	10367.98 $\pm$ 593.97	403.72 $\pm$ 88.67	16750.99 $\pm$ 714.70	16.01 $\pm$ 3.17
	2	25 < D $\leq$ 175	Paralarval stage	11558.32 $\pm$ 593.08	187.90 $\pm$ 27.92	16064.96 $\pm$ 659.79	12.36 $\pm$ 2.06
	3	175 < D $\leq$ 375	Juvenile stage	12000.01 $\pm$ 430.49	142.41 $\pm$ 24.72	14785.49 $\pm$ 315.72	10.47 $\pm$ 1.24
	4	375 < D $\leq$ 575	Sub-adult stage	11727.76 $\pm$ 574.31	92.50 $\pm$ 17.48	14604.96 $\pm$ 527.98	13.67 $\pm$ 2.26
	5	D > 575	Adult stage	11498.52 $\pm$ 577.13	72.84 $\pm$ 16.60	15887.13 $\pm$ 835.88	18.15 $\pm$ 2.35
Winter-spring cohort	1	D $\leq$ 25	Embryonic stage	10704.13 $\pm$ 521.00	350.51 $\pm$ 77.69	16783.21 $\pm$ 950.30	13.81 $\pm$ 2.66
	2	25 < D $\leq$ 175	Paralarval stage	12202.97 $\pm$ 744.46	164.03 $\pm$ 28.78	16111.13 $\pm$ 610.02	12.43 $\pm$ 1.80
	3	175 < D $\leq$ 325	Juvenile stage	12630.53 $\pm$ 538.05	136.57 $\pm$ 19.21	14800.37 $\pm$ 460.25	10.46 $\pm$ 1.54
	4	325 < D $\leq$ 525	Sub-adult stage	12248.32 $\pm$ 560.05	99.49 $\pm$ 14.78	14051.75 $\pm$ 481.17	12.57 $\pm$ 1.68
	5	D > 525	Adult stage	12146.32 $\pm$ 542.36	76.53 $\pm$ 14.13	14842.78 $\pm$ 507.97	17.59 $\pm$ 2.21

However, in the North Pacific, *O. bartramii* undergo extensive seasonal migration between spawning grounds in subtropical waters and feeding grounds in subpolar waters (Yatsu et al., 1998).

They spawn in subtropical waters with relatively higher water temperature. Hatched paralarvae start to migrate northward for food, and finally reach the subpolar waters with lower water





temperature (Wang et al., 2021). Thus, the U-trend of Sr/Ca cannot be explained by the temperature alone (Yatsu et al., 1998). In addition to temperature, feeding potentially affect Sr/Ca ratios (Zumholz et al., 2006). From juveniles to adults, they change their diet from crustaceans to fishes and squids (Murata, 1990). Their ratios vary with diet types, thus potentially masking the influences of environmental factors (Zumholz et al., 2006). In addition, the ratio of Sr/Ca had significant differences between winter-spring and autumn cohorts ( $P < 0.01$ ). When the individuals are in the same ontogenetic stage, different cohorts live in different seasons, and seasonal differences may result in relatively higher water temperatures in the habitat of winter-spring cohorts, which affect the Sr/Ca ratio of different cohorts. Different food types also impacts the Sr/Ca ratio of two cohorts (Zumholz et al., 2006; Liu et al., 2016). During the northward migration, winter-spring cohort mainly prey small pelagic fishes (*Cololabis saira*) and micronektonic squid (*Watasenia scintillans*), while autumn cohort mainly fed on squid (*Gonatus berryi* and *Berryteuthis anonychus*) and subtropical water myctophids (*Ceratoscopelus warmingi*, *Symbolophorus californiensis*, and *Electrona risso*) (Watanabe et al., 2004; Ichii et al., 2009; Fang et al., 2016a). Therefore, based on the above conclusions, it could be inferred that the difference in Sr/Ca ratio of two cohorts might be related to the seasonal change of water temperature and different diet types.

The Na/Ca ratio of the two cohorts fluctuated greatly at different stages, and the Na/Ca ratio had significant differences between two cohorts, which might be related to the water environment, food composition, element deposition mechanism and organ development degree of different cohorts in different stages, and the strength of individual respiration and metabolism also affect the absorption of elements (Zumholz et al., 2006; Liu et al., 2011a,b). The food composition, water temperature, and physiological conditions of the two cohorts will change from juveniles to adults (Bower and Ichii, 2005; Ichii et al., 2009), which may result the Na/Ca ratio of the two cohorts fluctuated greatly. Due to the different habitats of different cohorts, the changes of

these factors are also different (Bower and Ichii, 2005), which may lead to the difference of Na/Ca ratio between the two cohorts. However, we are not quite clear about how these factors affected the Na/Ca ratio, so we should strengthen the research in this aspect in the later research.

## Differentiation of Migration Routes

The movement pattern of squid is closely related to the surrounding environment (Liu et al., 2016). Juveniles of squid has weak swimming capabilities and mainly drifts passively with the movement of the ocean current (Liu et al., 2016; Fang et al., 2019). When they grow to a certain stage, they will actively migrate for a long distance in order to feed and spawn (Fang et al., 2019; Li et al., 2021). Current is the main factor that determines the passive movement of squid, while feeding and spawning are important factors that determine the active movement (Liu et al., 2016; Fang et al., 2019; Li et al., 2021). Therefore, the reconstruction of migration routes of squid can improve our understanding of population dynamics and growth characteristics, and provide a reference for resource assessment and management of this species.

Based on the MRT model, five clusters were identified through chronological clustering. Combined with the age study of *O. bartramii* (Chen and Chiu, 2003; Fang et al., 2019), the time period of the five clusters could be defined as the five life stages in the process of ontogeny: embryonic stage, paralarval stage, juvenile stage, sub-adult stage, and adult stage. By analyzing the element of different ontogenetic stages and combining environmental factors, the migration routes of different cohorts of *O. bartramii* can be reconstructed. Studies have shown that water temperature was an important environmental factor affecting the growth and distribution of squid (Gillanders et al., 2013; Li et al., 2021). In previous studies, only SST was selected to study migration route (Liu et al., 2016; Fang et al., 2019). However, squid perform vertical migrations, and the temperature of different water layers also affects its distribution. Therefore, this study selected the temperature of different water

layers (Temp<sub>100</sub> and SST) to explore the migration routes of *O. bartramii*.

Studies have shown that both the winter-spring and autumn cohorts migrated from spawning grounds in subtropical waters to feeding grounds in subarctic waters (Ichii et al., 2009), which is consistent with the results shown in this study. However, there were differences in the habitats of different cohorts at different stages. This study showed that the range of highest probability occurrence of embryonic stage between autumn and winter-spring cohorts was different, and the range of the autumn cohort was 28–33°N, 163–175°E, the range of the winter-spring cohort was 22–30°N, 132–160°E. Ichii et al. (2009) described that the optimum spawning SST range for *O. bartramii* underwent seasonal movements to the south during winter and to the north in summer. As a result, the latitude of the spawning ground of the autumn cohort is higher than that of the winter-spring cohort. It is known that squid at the early life stage (e.g., egg, paralarvae, and even juvenile) lack the ability to actively swim and only passively move with the currents (Ichii et al., 2009; Nishikawa et al., 2014, 2015). In autumn, Kuroshio extension current (KEF) has higher average eastward velocity at 33–37°N (Ichii et al., 2009). As the current moves, the eggs, paralarvae, and juveniles of the autumn cohort passively move eastward. During the sub-adult and adult stage, the squid continued to move to the northeast to feed and migrated to the subarctic border waters in May (Fang et al., 2019). Finally, fishing vessel caught squid at 39–42°N from May to July. The migration of the winter-spring cohort is also affected by the Kuroshio Current (Fang et al., 2019). Watanabe et al. (2008) indicated that for the winter-spring cohort of *O. bartramii* to actively prey on its food in summer, this migration orientation would be influenced by the Kuroshio and Kuroshio Extension that transports some individuals to an offshore area (eastward to 150°E) (Nishikawa et al., 2014), which is consistent with the results shown in this study. The highest probability occurrence of sub-adult stage reached 40°N, which is the Kuroshio–Oyashio transition and Kuroshio regions and has a prey-rich environment (Watanabe et al., 2008). Therefore, it is the highest probability of nursery grounds for *O. bartramii* (Ichii et al., 2009). The squid continued to move to the north and reached 40–45°N at adult stage. After October and November, *O. bartramii* reached the peak of sexual maturity and began to migrate to the south (Ichii et al., 2009; Fang et al., 2019), which is confirmed by squid caught at 39°N in November.

## CONCLUSION

We analyzed the composition and concentration of elements in *O. bartramii* statolith of different cohorts, and reconstructed their migration route based on the relationship between water temperature and the ratios of key trace elements to Ca. The reconstructed migration route was roughly consistent with previous studies, which presented a northward migration from spawning grounds in subtropical waters to feeding grounds in subarctic waters. The growth of the squid is not only affected by water temperature, but also by currents, food, salinity, etc. Climate events (El Niño and La Niña events, etc.) also affect the distribution of its habitat. Therefore, we can try to add other

environmental factors to explore the migration routes of squid or explore the difference in the migration routes of different years in the future research. In addition, in future research, we can also combine stable isotopes ( $\delta^{13}\text{C}$  and  $\delta^{15}\text{N}$ ) to trace the source and feeding route of individual to determine the habitat distribution. Based on the above methods, a more comprehensive and complete migration routes of *O. bartramii* will be further reconstructed to provide more effective new information for the resource management.

In addition, our fishing location is located in the feeding ground for *O. bartramii*, we can only get the migration route of *O. bartramii* from the spawning ground to the feeding ground. However, the route of migration from feeding grounds to spawning grounds is not clear. In future research, we hope to overcome this difficulty by changing the fishing location, so as to achieve the reconstruction of the complete route of *O. bartramii*.

## DATA AVAILABILITY STATEMENT

The original contributions presented in the study are included in the article/**Supplementary Material**, further inquiries can be directed to the corresponding author.

## ETHICS STATEMENT

The animal study was reviewed and approved by Ethics Committee of Shanghai Ocean University.

## AUTHOR CONTRIBUTIONS

PH: methodology, software, writing, and original draft preparation. ZF: software and validation. NL: methodology, software, and reviewing. XC: writing, reviewing, and editing. All authors contributed to the article and approved the submitted version.

## FUNDING

This work was funded by the National Key R&D Program of China (2019YFD0901404), National Nature Foundation of China on the project (NSFC41876141), and Funding for the Opening of Key Laboratories for Offshore Fishery Development by the Ministry of Agriculture (LOF 2021-01).

## ACKNOWLEDGMENTS

The support from the captains and crews in commercial jigging vessels in scientific surveys is gratefully acknowledged.

## SUPPLEMENTARY MATERIAL

The Supplementary Material for this article can be found online at: <https://www.frontiersin.org/articles/10.3389/fmars.2022.832639/full#supplementary-material>

## REFERENCES

- Akaike, H. (1974). A new look at the statistical model identification. *IEEE Trans. Automat. Contr.* 19, 716–723. doi: 10.1109/TAC.1974.1100705
- Alabia, I. D., Saitoh, S. I., Igarashi, H., Ishikawa, Y., and Imamura, Y. (2020). Spatial Habitat Shifts of Oceanic Cephalopod (*Ommastrephes bartramii*) in Oscillating Climate. *Remote Sens.* 12:521. doi: 10.3390/rs12030521
- Arkhipkin, A. I. (2005). Staloliths as 'black boxes' (life recorders) in squid. *Mar. Freshw. Res.* 56, 573–583. doi: 10.1071/MF04158
- Arkhipkin, A. I. (2013). Squid as nutrient vectors linking Southwest Atlantic marine ecosystems. *Deep Sea Res. II Top. Stud. Oceanogr.* 95, 7–20. doi: 10.1016/j.dsr2.2012.07.003
- Arkhipkin, A. I., Campana, S. E., FitzGerald, J., and Thorrold, S. R. (2004). Spatial and temporal variation in elemental signatures of staloliths from the Patagonian longfin squid (*Loligo gahi*). *Can. J. Fish. Aquat. Sci.* 61, 1212–1224. doi: 10.1139/f04-075
- Arkhipkin, A. I., Hendrickson, L. C., Ignacio, P., Pierce, G. J., Roa-Ureta, R. H., Robin, J. P., et al. (2021). Stock assessment and management of cephalopods: advances and challenges for short-lived fishery resources. *ICES J. Mar. Sci.* 78, 714–730. doi: 10.1093/icesjms/fsaa038
- Bettencourt, V., and Guerra, A. (2000). Growth increments and biomineralization process in cephalopod staloliths. *J. Exp. Mar. Biol. Ecol.* 248, 191–205. doi: 10.1016/S0022-0981(00)00161-1
- Bower, J. R., and Ichii, T. (2005). The red flying squid (*Ommastrephes bartramii*): a review of recent research and the fishery in Japan. *Fish. Res.* 76, 39–55. doi: 10.1016/j.fishres.2005.05.009
- Bower, S. M., and Margolis, L. (1991). Potential use of helminth parasites in stock identification of flying squid, *Ommastrephes bartramii*, in North Pacific waters. *Can. J. Zool.* 69, 1124–1126. doi: 10.1139/z91-158
- Campana, S. E., and Neilson, J. D. (1985). Microstructure of fish otoliths. *Can. J. Fish. Aquat. Sci.* 42, 1014–1032. doi: 10.1139/f85-127
- Chan, L., Drummond, D., Edmond, J., and Grant, B. (1997). On the barium data from the Atlantic GEOSECS expedition. *Deep Sea Res.* 24, 613–649. doi: 10.1016/0146-6291(77)90505-7
- Chen, C. S. (2010). Abundance trends of two neon flying squid (*Ommastrephes bartramii*) stocks in the North Pacific. *ICES J. Mar. Sci.* 67, 1336–1345. doi: 10.1093/icesjms/fsq063
- Chen, C. S., and Chiu, T. S. (2003). Variations of life history parameters in two geographical groups of the neon flying squid, *Ommastrephes bartramii*, from the North Pacific. *Fish. Res.* 63, 349–366. doi: 10.1016/S0165-7836(03)00101-2
- Chen, X. J., Liu, B. L., and Chen, Y. (2008). A review of the development of Chinese distant-water squid jigging fisheries. *Fish. Res.* 89, 211–221. doi: 10.1016/j.fishres.2007.10.012
- Dilly, P. N. (1977). The structure of some cephalopod staloliths. *Cell Tissue Res.* 175, 147–163. doi: 10.1007/BF00232076
- Fang, Z., Han, P. W., Wang, Y., Chen, Y. Y., and Chen, X. J. (2021). Interannual variability of body size and beak morphology of the squid *Ommastrephes bartramii* in the North Pacific Ocean in the context of climate change. *Hydrobiologia* 848, 1295–1309. doi: 10.1007/s10750-021-04528-7
- Fang, Z., Liu, B. L., Chen, X. J., and Chen, Y. (2019). Ontogenetic difference of beak elemental concentration and its possible application in migration reconstruction for *Ommastrephes bartramii* in the North Pacific Ocean. *Acta Oceanol. Sin.* 38, 43–52. doi: 10.1007/s13131-019-1431-5
- Fang, Z., Thompson, K., Jin, Y., Chen, X. J., and Chen, Y. (2016a). Preliminary analysis of beak stable isotopes ( $\delta^{13}\text{C}$  and  $\delta^{15}\text{N}$ ) stock variation of neon flying squid, *Ommastrephes bartramii*, in the North Pacific Ocean. *Fish. Res.* 177, 153–163. doi: 10.1016/j.fishres.2016.01.011
- Fang, Z., Li, J. H., Thompson, K., Hu, F. F., Chen, X. J., Liu, B. L., et al. (2016b). Age, growth, and population structure of the red flying squid (*Ommastrephes bartramii*) in the North Pacific Ocean, determined from beak microstructure. *Fish. Bull.* 114, 34–44. doi: 10.7755/FB.114.1.3
- Gillanders, B. M. (2005). Using elemental chemistry of fish otoliths to determine connectivity between estuarine and coastal habitats. *Estuar. Coast. Shelf Sci.* 64, 47–57. doi: 10.1016/j.ecss.2005.02.005
- Gillanders, B. M., Wilkinson, L. M., Munro, A. R., and de Vries, M. C. (2013). Stalolith chemistry of two life history stages of cuttlefish: effects of temperature and seawater trace element concentration. *Geochim. Cosmochim. Acta* 101, 12–33. doi: 10.1016/j.gca.2012.10.005
- Han, P. W., Wang, Y., Fang, Z., and Chen, X. J. (2022). Response of daily increment of stalolith of neon flying squid (*Ommastrephes bartramii*) for different cohorts to marine environment in the North Pacific. *Haiyang Xuebao* 44, 112–128.
- Hu, G. Y., Chen, X. J., Liu, B. L., and Fang, Z. (2015). Microstructure of stalolith and beak for *Dosidicus gigas* and its determination of growth increments. *J. Fish. China* 39, 361–369.
- Hu, Z. C., Gao, S., Liu, Y. S., Hu, S., Chen, H., and Yuan, H. (2008). Signal enhancement in laser ablation ICP-MS by addition of nitrogen in the central channel gas. *J. Anal. At. Spectrom.* 23, 1093–1101. doi: 10.1039/b804760j
- Hüssy, K., Limburg, K. E., de Pontual, H., Thomas, O. R., Cook, P. K., Heimbrand, Y., et al. (2020). Trace Element Patterns in Otoliths: the Role of Biomineralization. *Rev. Fish. Sci. Aquac.* 29, 445–477. doi: 10.1080/23308249.2020.1760204
- Ichii, T., Mahapatra, K., Sakai, M., and Okada, Y. (2009). Life history of the neon flying squid: effect of the oceanographic regime in the North Pacific Ocean. *Mar. Ecol. Prog. Ser.* 378, 1–11. doi: 10.3354/meps07873
- Jones, J. B., Arkhipkin, A. I., Marriott, A. L., and Pierce, G. J. (2019). Reprint of using stalolith elemental signatures to confirm ontogenetic migrations of the squid *Doryteuthis gahi* around the Falkland Islands (Southwest Atlantic). *Chem. Geol.* 526, 165–174. doi: 10.1016/j.chemgeo.2018.04.002
- Li, N., Fang, Z., Chen, X. J., and Feng, Z. P. (2021). Preliminary study on the migration characteristics of swordtip squid (*Uroteuthis edulis*) based on the trace elements of stalolith in the East China Sea. *Reg. Stud. Mar. Sci.* 46:101879. doi: 10.1016/j.rsma.2021.101879
- Lipinski, M. R., and Underhill, L. G. (1995). Sexual maturation in squid: quantum or continuum. *S. Afr. J. Mar. Sci.* 15, 207–223. doi: 10.2989/02577619509504844
- Lischka, A., Braid, H. E., Pannell, J. L., Pook, C. J., Gaw, S., Yoo, M., et al. (2020). Regional assessment of trace element concentrations in arrow squids (*Nototodarus gouldi*, *N. sloanii*) from New Zealand waters: bioaccessibility and impact on food web and human consumers. *Environ. Pollut.* 264:114662. doi: 10.1016/j.envpol.2020.114662
- Lishchenko, F., Perales-Raya, C., Barrett, C., Oesterwind, D., Power, A. M., Larivain, A., et al. (2021). A review of recent studies on the life history and ecology of European cephalopods with emphasis on species with the greatest commercial fishery and culture potential. *Fish. Res.* 236:105847. doi: 10.1016/j.fishres.2020.105847
- Liu, B. L., Cao, J., Truesdell, S. B., Chen, Y., Chen, X. J., and Tian, S. Q. (2016). Reconstructing cephalopod migration with stalolith elemental signatures: a case study using *Dosidicus gigas*. *Fish. Sci.* 82, 425–433. doi: 10.1007/s12562-016-0978-8
- Liu, B. L., Chen, X. J., Lu, H. J., and Ma, J. (2011b). *Cephalopod Stalolith*. Beijing: Ocean Press, 23–160.
- Liu, B. L., Chen, X. J., Chen, Y., Lu, H. J., and Qian, W. G. (2011a). Trace Elements in the Staloliths of Jumbo Flying Squid Off the Exclusive Economic Zones of Chile and Peru. *Mar. Ecol. Prog. Ser.* 429, 93–101. doi: 10.3354/meps09106
- Liu, B. L., Chen, X. J., Chen, Y., and Tian, S. Q. (2013). Geographic variation in stalolith trace elements of the Humboldt squid, *Dosidicus gigas*, in high seas of Eastern Pacific Ocean. *Mar. Biol.* 160, 2853–2862. doi: 10.1007/s00227-013-2276-7
- Liu, B. L., Chen, Y., and Chen, X. J. (2015). Spatial difference in elemental signatures within early ontogenetic stalolith for identifying Jumbo flying squid natal origins. *Fish. Oceanogr.* 24, 335–356. doi: 10.1111/fog.12112
- Liu, Y., Hu, Z., Gao, S., Günther, D., Xu, J., Gao, C., et al. (2008). In situ analysis of major and trace elements of anhydrous minerals by LA-ICP-MS without applying an internal standard. *Chem. Geol.* 257, 34–43. doi: 10.1016/j.chemgeo.2008.08.004
- Lu, H. J., Chen, X. J., and Fang, Z. (2015). An analysis of element composition in the staloliths of *Illex argentisus* squid in the Southwest Atlantic Ocean. *Acta Ecol. Sin.* 35, 297–305. doi: 10.5846/stxb201303260514
- Lu, H. J., Chen, X. J., and Ma, J. (2014). Trace elements in the staloliths of neon flying squid, *Ommastrephes bartramii* in the Northwest Pacific Ocean. *Chin. J. Appl. Ecol.* 25, 2411–2417.
- Lu, H. J., Chen, Z. Y., and Tong, Y. H. (2019). Element composition in the staloliths of *Sthenoteuthis oualaniensis* squid in Xisha islands waters of South China Sea. *Chin. J. Appl. Ecol.* 30, 653–660. doi: 10.13287/j.1001-9332.201902.029

- Lu, H. J., Liu, B. L., Chen, X. J., and Fang, Z. (2013). Trace elements in the statoliths of *Dosidicus gigas* in the high sea waters off Chile. *Mar. Fish.* 35, 269–277.
- Mereu, M., Agus, B., Cannas, R., Cau, A., Coluccia, E., and Cuccu, D. (2015). Mark–recapture investigation on *Octopus vulgaris* specimens in an area of the central western Mediterranean Sea. *J. Mar. Biol. Assoc. U. K.* 95, 131–138. doi: 10.1017/S002531541400112X
- Morris, C. C. (1991). Statocyst fluid composition and its effects on calcium carbonate precipitation in the squid *Alloteuthis subulata* (Lamarck, 1798): towards a model for biomineralization. *Bull. Mar. Sci.* 49, 379–388.
- Murata, M. (1990). Oceanic resources of squids. *Mar. Behav. Physiol.* 18, 19–71. doi: 10.1080/10236249009378779
- Nishikawa, H., Igarashi, H., Ishikawa, Y., Sakai, M., Kato, Y., Ebina, M., et al. (2014). Impact of paralarvae and juveniles feeding environment on the neon flying squid (*Ommastrephes bartramii*) winter–spring cohort stock. *Fish. Oceanogr.* 23, 289–303. doi: 10.1111/fog.12064
- Nishikawa, H., Toyoda, T., Masuda, S., Ishikawa, Y., Sasaki, Y., Igarashi, H., et al. (2015). Wind-induced stock variation of the neon flying squid (*Ommastrephes bartramii*) winter–spring cohort in the subtropical North Pacific Ocean. *Fish. Oceanogr.* 24, 229–241. doi: 10.1111/fog.12106
- O’Dor, R. K., and Balch, N. (1985). Properties of *Illex illecebrosus* egg masses potentially influencing larval oceanographic distribution. *NAFO Sci. Coun. Stud.* 9, 69–76.
- Pan, X. D., Ye, Z. J., Xu, B. D., Jiang, T., Yang, J., Cheng, J., et al. (2020). Combining otolith elemental signatures with multivariate analytical models to verify the migratory pattern of Japanese Spanish mackerel (*Scomberomorus niphonius*) in the southern Yellow Sea. *Acta Oceanol. Sin.* 39, 54–64. doi: 10.1007/s13131-020-1606-0
- R Development Core Team (2019). *R: A Language and Environment for Statistical Computing*. Vienna: R Foundation for Statistical Computing.
- Radtke, R. (1983). Chemical and structural characteristics of statoliths from the shortfinned squid *Illex illecebrosus*. *Mar. Biol.* 76, 47–54. doi: 10.1007/bf00393054
- Santos, M. B., Clarke, M. R., and Pierce, G. J. (2001). Assessing the importance of cephalopods in the diets of marine mammals and other top predators: problems and solutions. *Fish. Res.* 52, 121–139. doi: 10.1016/S0165-7836(01)00236-3
- Semmens, J. M., Pecl, G. T., Gillanders, B. M., Waluda, C. M., Shea, E. K., Jouffre, D., et al. (2007). Approaches to resolving cephalopod movement and migration patterns. *Rev. Fish Biol. Fish.* 17, 401–423. doi: 10.1007/s11160-007-9048-8
- Sun, L. L., He, M. S., Chi, C. F., Zhou, L., Liu, H. H., and Shi, H. L. (2015). Progress on cephalopods statoliths structure analysis and its applications. *J. Zhejiang Ocean Univ.* 34, 479–485.
- Tanaka, H. (2001). Tracking the neon flying squid by the biotelemetry system, in the central North Pacific Ocean. *Aquabiology* 23, 533–539.
- Vijai, D., Sakai, M., and Sakurai, Y. (2015). Embryonic and paralarval development following artificial fertilization in the neon flying squid *Ommastrephes bartramii*. *Zoomorphology* 134, 417–430. doi: 10.1007/s00435-015-0267-6
- Wang, J. T., Cheng, Y. Q., Lu, H. J., Chen X. J., Lin, L., and Zhang, J. B. (2022). Water temperature at different depths affects the distribution of neon flying squid (*Ommastrephes bartramii*) in the Northwest Pacific Ocean. *Front. Mar. Sci.* 8:741620. doi: 10.3389/fmars.2021.741620
- Wang, Y., Han, P. W., Fang, Z., and Chen, X. J. (2021). Climate-induced life cycle and growth variations of neon flying squid (*Ommastrephes bartramii*) in the North Pacific Ocean. *Aquac. Fish.* doi: 10.1016/j.aaf.2021.08.006
- Watanabe, H., Kubodera, T., Ichii, T., and Kawahara, S. (2004). Feeding habits of neon flying squid *Ommastrephes bartramii* in the transitional region of the central North Pacific. *Mar. Ecol. Prog. Ser.* 266, 173–184. doi: 10.3354/meps266173
- Watanabe, H., Kubodera, T., Ichii, T., Sakai, M., Moku, M., and Seitou, M. (2008). Diet and sexual maturation of the neon flying squid *Ommastrephes bartramii* during autumn and spring in the Kuroshio–Oyashio transition region. *J. Mar. Biol. Assoc. U. K.* 88, 381–389. doi: 10.1017/S0025315408000635
- Wearmouth, V. J., Durkin, O. C., Bloor, I. S. M., McHugh, M. J., Rundle, J., and Sims, D. W. (2013). A method for long-term electronic tagging and tracking of juvenile and adult European common cuttlefish *Sepia officinalis*. *J. Exp. Mar. Biol. Ecol.* 447, 149–155. doi: 10.1016/j.jembe.2013.02.023
- Xiong, Y., Liu, H. B., Tang, J. H., Zhong, X. M., Liu, P. T., Yang, J., et al. (2015). Application of otolith microchemistry on reconstruction of migratory patterns and cohort discrimination in marine fishes. *Chin. Bull. Life Sci.* 27, 953–959.
- Xu, W., Chen, X. J., Liu, B. L., Chen, Y., Cao, L. L., and Huan, M. Y. (2020). Discrimination of geographical population of jumbo flying squid (*Dosidicus gigas*) using the trace elements in the nuclear part of eye lenses. *J. Fish. China* 44, 947–958. doi: 10.11964/jfc.20190411753
- Yamaguchi, T., Kawakami, Y., and Matsuyama, M. (2018). Analysis of the hatching site and migratory behaviour of the swordtip squid (*Uroteuthis edulis*) caught in the Japan Sea and Tsushima Strait in autumn estimated by statolith analysis. *Mar. Biol. Res.* 14, 105–112. doi: 10.1080/17451000.2017.1351616
- Yatsu, A., Midorikawa, S., Shimada, T., and Uozumi, Y. (1997). Age and growth of the neon flying squid, *Ommastrephes bartramii*, in the North Pacific Ocean. *Fish. Res.* 29, 257–270. doi: 10.1016/S0165-7836(96)00541-3
- Yatsu, A., Mochioka, N., Morishita, K., and Toh, H. (1998). Strontium/Calcium ratios in statoliths of the neon flying squid, *Ommastrephes bartramii* (Cephalopoda), in the North Pacific Ocean. *Mar. Biol.* 131, 275–282. doi: 10.1007/s002270050320
- Yu, W., Chen, X. J., Chen, Y., Yi, Q., and Zhang, Y. (2015). Effects of environmental variations on the abundance of western winter–spring cohort of neon flying squid (*Ommastrephes bartramii*) in the Northwest Pacific Ocean. *Acta Oceanol. Sin.* 34, 43–51. doi: 10.1007/s13131-015-0707-7
- Yu, W., Chen, X. J., Yi, Q., Gao, G. P., and Chen, Y. (2016). Impacts of climatic and marine environmental variations on the spatial distribution of *Ommastrephes bartramii* in the Northwest Pacific Ocean. *Acta Oceanol. Sin.* 35, 108–116. doi: 10.1007/s13131-016-0821-1
- Yu, W., Chen, X. J., Yi, Q., and Li, Y. S. (2013). Review on the early life history of neon flying squid *Ommastrephes bartramii* in the North Pacific. *J. Shanghai Ocean Univ.* 22, 755–762.
- Zumholz, K., Hansteen, T. H., Klügel, A., and Piatkowski, U. (2006). Food effects on statolith composition of the common cuttlefish (*Sepia officinalis*). *Mar. Biol.* 150, 237–244. doi: 10.1007/s00227-006-0342-0
- Zumholz, K., Klügel, A., Hansteen, T., and Piatkowski, U. (2007). Statolith microchemistry traces the environmental history of the boreoatlantic armhook squid *Gonatus fabricii*. *Mar. Ecol. Prog. Ser.* 333, 195–204. doi: 10.3354/meps333195

**Conflict of Interest:** The authors declare that the research was conducted in the absence of any commercial or financial relationships that could be construed as a potential conflict of interest.

**Publisher’s Note:** All claims expressed in this article are solely those of the authors and do not necessarily represent those of their affiliated organizations, or those of the publisher, the editors and the reviewers. Any product that may be evaluated in this article, or claim that may be made by its manufacturer, is not guaranteed or endorsed by the publisher.

Copyright © 2022 Han, Fang, Li and Chen. This is an open-access article distributed under the terms of the Creative Commons Attribution License (CC BY). The use, distribution or reproduction in other forums is permitted, provided the original author(s) and the copyright owner(s) are credited and that the original publication in this journal is cited, in accordance with accepted academic practice. No use, distribution or reproduction is permitted which does not comply with these terms.